Journal of Molecular Structure 1108 (2016) 235–244

Contents lists available at ScienceDirect

Journal of Molecular Structure

journal homepage: http://www.elsevier.com/locate/molstruc

Influence of methoxy-substituents on the strength of Br ··· Br type II halogen bonds in bromobenzoic acid

Pablo A. Raffo [a], Juan P. Marcolongo [a], Alejandro V. Funes [a], Leonardo D. Slep [a], Ricardo F. Baggio [b], Fabio D. Cukiernik [a, *]

[a] DQIAQF-INQUIMAE, Facultad de Ciencias Exactas y Naturales Universidad de Buenos Aires Pabello II – Cdad. Universitaria – Nuñez C1428EGA, CABA, Argentina

[b] Gerencia de Investigación y Aplicaciones, Centro Atómico Constituyentes, Comisión Nacional de Energía Atómica, Buenos Aires, Argentina

ARTICLE INFO

Article history:
Received 1 November 2015
Received in revised form
4 December 2015
Accepted 4 December 2015
Available online 11 December 2015

Keywords:
Alkoxy-substituted benzoic acids
Rationalization of packing modes
Halogen bonds
Type II Br ··· Br contact

ABSTRACT

4-bromo-3,5-di(methoxy)benzoic acid (**I**) crystallizes in the monoclinic C2/c space group, a = 22.3405 (6) Å, b = 4.85142 (14) Å, c = 18.1583 (5) Å, β = 93.086 (2)°. The crystal structure shows head-to-head dimeric units linked via type II Br ··· Br interactions as well as Br ··· π and weak H-bonding interactions. The whole structure exhibits features similar to those of the parent 4-bromobenzoic acid (**II**), most notably the overall geometrical features involved in the Br ··· Br type II interactions. Both structures display comparable C–Br ··· Br angles (θ_1 = 98.3 and 91.6° and θ_2 = 163.0 and 163.5° for (**I**) and (**II**) respectively), but the Br ··· Br distance is significantly shorter in (**I**) (3.58 Å) than in (**II**) (3.81 Å). QM computations provide the magnitude of the intermolecular interactions present in both (**I**) and (**II**), and allow disclosing the individual covalent and electrostatic contributions to the Br···Br halogen bond in terms of interaction energies, electrostatic potentials, and a molecular orbital (MO) analysis.

1. Introduction

Halogen bond (XB) has become in recent years one of the most intensively investigated intermolecular interactions due to its relevance in crystal engineering, molecular recognition and molecular design of supramolecular materials [1–6]. A deep understanding of the nature of XB is a target in itself: this knowledge could provide more reliable tools for the design of functional materials and help assessing fundamental concepts concerning non-covalent interactions -including competitive and cooperative cases-while promoting the development of experimental and computational techniques [7–13].

Recent work on this subject involved both experimental (mainly crystallographic) and computational studies aimed to rationalize the influence of different molecular fragments on the strength and geometrical features of this interaction [2,3,14]. Complementary, some computational reports started to explore the relative contribution of the electrostatic and covalent components to the whole interaction [2,8,15–17]. The vast majority of these studies involved $R_{don}C\text{-}X \cdots Nu\text{-}R_{acc}$ interacting pairs in which X is Cl, Br or I and Nu stands for O- or N-based nucleophiles (bases) (R_{don} denotes a chemical group attached to the halogen-donor moiety while R_{acc} is linked to the halogen-acceptor moiety). The influence of the nature of both the halogen atom X and the substituents present on R_{don} and R_{acc} has been rationalized in terms of the σ acidity of X [3,7,18,19] and the lone-pair availability on Nu [3,18–21]. Note that in most cases the substituents on R_{don} were other halogen groups. However, studies involving X-based nucleophiles (i.e.: systems in which the halogen acceptor is also a halogen atom attached to a chemical group) are much more restricted [10,22,23]. Only recently type II X ··· X contacts (Scheme 1) have been fully accepted as true (donor-acceptor) XB [12,24,25].

Comparisons along the Cl – Br – I series point to the importance of the polarizability of the atoms in determining the properties and structural trends of the XB bonds. A comprehensive computational study on Br···Br interactions has recently been published [23]. Nevertheless, there are still many aspects to be explored and, as stated by Mukherjee and Desiraju [10], "the nature of Br remains blurred and any study to this end would be useful to the future application of halogen bonds".

We decided to explore the effect of non-halogen substituents in R_{don} on type II X ··· X bonds. For this purpose we employed non-

* Corresponding author. Tel.: +54 1145763358; fax:+54 1145763341.
E-mail address: fabioc@qi.fcen.uba.ar (F.D. Cukiernik).

http://dx.doi.org/10.1016/j.molstruc.2015.12.016
0022-2860/

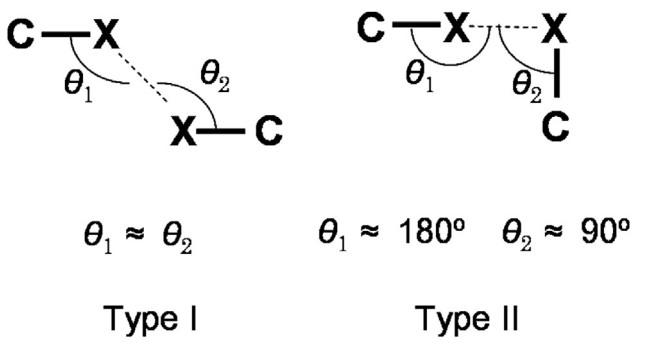

Scheme 1. X ··· X short contacts: type I arise essentially from close packing; type II have a more chemical (donor-acceptor) sense.

halogen atoms attached to a "benzoic acid platfom" –specifically a "bromobenzoic acid platform". Derivatives based on benzoic acid have a strong tendency to crystallize. The factors governing their supramolecular organization, even in the presence of competitive interactions, are well understood. Substitutions at different positions are relatively easy to achieve allowing for a fine tuning of the electron distribution around the Br center. Type II Br ··· Br halogen bond has been found to be an efficient supramolecular organizer of cocrystals of Br-benzamide (closely related to Br-benzoic acids) with aliphatic dicarboxylic acids [25], where the concept of *synthon modularity* worked very well. Specifically, a Conquest search in the CSD for the 4-bromobenzoic acid substructure retrieved 26 cases including cocrystals. In all of them the head-to-head dimeric synthon, or the related synthon derived from the interaction of the carboxyl group with bases like pyrazine or 4,4′-bipyridine is the essential structural building block. In most cases, these synthons organize in parallel lamellae as a consequence of π-π and C—H ··· O interactions. Only 4 entries show "nearly perpendicular" arrangements based on type II Br ··· Br interactions; three of them (BRBZAP, BRBZAP01 and BRBZAP02) correspond to 4-bromobenzoic acid itself [26]. Five structures exhibit type I Br ··· Br contacts with almost identical θ_1 and θ_2 angles (BOTVUC, GOLLOI, WOKWOK, TUSQUT, YAKSUN).

We selected alkoxy-chains to play the role of non-halogen substituents. They are expected to act as π-electron donors and we are quite familiar with the effect they can exert on the structures of substituted benzoic acids [27], which are similar to those established for propiolic and cynammic acids [28]. OH groups have been discarded because they could introduce strong OH ··· O interactions that might prevail as organizers as shown in the case of 4-bromo-3,5-di(hydroxy)benzoic acid monohydrate [29]. Among the alkoxy-substituents, we have shown recently that the methoxy-groups at the 3,5- positions do not interfere with the supramolecular organization of benzoic acid, whereas longer chains like ethoxy-groups do [27].

We thus report in this manuscript the crystal structure of 4-bromo-3,5-di(methoxy)benzoic acid (**I**) (Scheme 2) and compare it with the already known structure of the parent 4-bromobenzoic acid (**II**). The interactions giving rise to their structures are analyzed in terms of both geometrical considerations and quantum mechanical computations aimed to estimate their magnitudes. Along this analysis we focus our attention on the relative strengths of the Br ··· Br halogen bond interactions and discuss the effect of the introduction of the methoxy-groups.

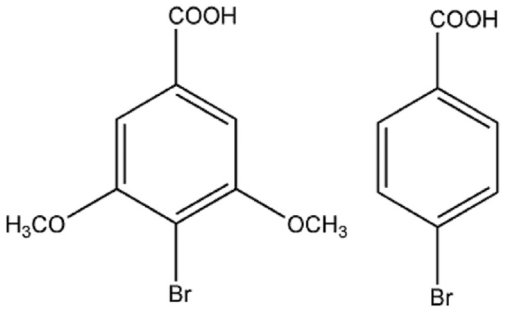

Scheme 2. Chemical sketch of compounds (**I**) (left) and (**II**) (right).

2. Experimental

2.1. Crystallization

4-bromo-3,5-di(methoxy)benzoic acid has been purchased from Sigma–Aldrich and used without further purification. Single crystals for data acquisition were selected by optical inspection under polarized light from crops obtained by very slow cooling (cooling rate below 1 K day^{-1}) of concentrated acetonitrile solutions of (**I**).

2.2. X-ray crystallography

Crystal Data were collected on an Oxford Gemini CCD S Ultra diffractometer at room temperature using Mo Kα radiation (λ = 0.71073 Å) [30]. The structure was solved by direct methods and refined by full-matrix least squares on F^2 using the SHELXS-97 software [31]. All non-hydrogen atoms were refined anisotropically with SHELXL-2014 [32]. The structural analysis was performed with the help of the multipurpose PLATON program [33] and the molecular representations shown in the figures were generated using XP in the SHELXTL package [31]. Crystallographic data (excluding structure factors) for the structures in this paper have been deposited with the Cambridge Crystallographic Data Centre as supplementary publication # CCDC 1418932. Copies of the data can be obtained, free of charge, on application to CCDC, 12 Union Road, Cambridge CB2 1EZ, UK, (fax: +44 1223 336033 or e-mail: deposit@ccdc.cam.ac.uk).

All H atoms were found in a difference map, C—H's being further idealized and finally allowed to ride, while the carboxylic H was refined with a restrained O—H distance. CH_3 groups were in turn allowed to rotate. Displacement parameters were taken as $U_{iso}(H) = X \times U_{eq}(Host)$ [Parameters used: $(C–H)_{methyl}$ = 0.96 Å, X = 1.5; d(C—H)$_{arom}$ = 0.93 Å, X = 1.2, d(O—H) = 0.85 (1) Å, X = 1.2].

2.3. Quantum mechanical calculations

We employed Density functional Theory (DFT) to explore the magnitude (and nature) of the interactions between pairs of molecules in both molecular systems compared in this report. In all cases single point (SP) computations at the experimental geometries were performed with Gaussian 09 [34], employing the M06-2X functional and the 6-311 + G(d,p) basis set implemented in Gaussian 09, a combination that proved adequate in the past to explore other related systems [8]. As basis set superposition errors (BSSE) are expected to introduce deviations when computing the interaction energies between weakly bound fragments [35,36], we performed in vacuo SP computations of the individual moieties and the interacting assemblies, and performed a counterpoise correction [37,38]. Both evaluations lead to essentially the same qualitative conclusions, and are included for completeness in Fig. 5,

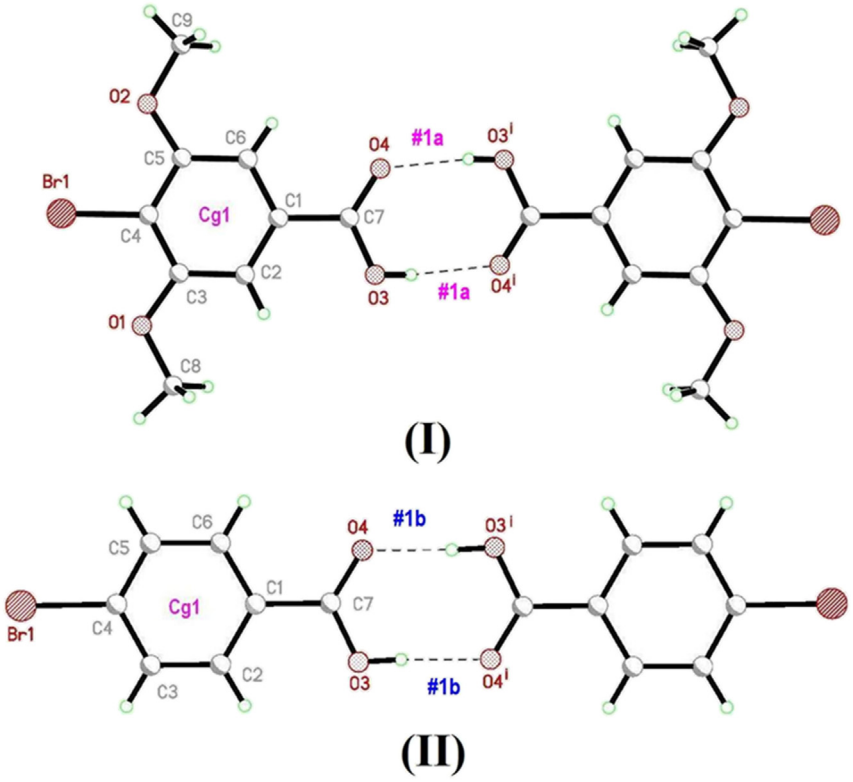

Fig. 1. The dimeric units in (**I**), (**II**), with atom labeling. (For symmetry codes see Tables 2–5).

though only the corrected values are employed throughout the text.

The Br … Br interaction between individual molecules was also explored by means of quantitative molecular orbital (MO) picture. This representation allows for a chemically intuitive detection of the covalent interaction between the constituting monomeric fragments. The computations involve: (i) SP evaluations of the isolated and the interacting systems, which provide the MO's of the interacting pair as linear combinations of the gaussian basis functions selected for the calculations. (ii) Evaluation of the MO's of the non-bonded individual fragments at their crystallographic geometry keeping the mutual electrostatic influence. For this purpose, each fragment was alternatively substituted in a self-consistent procedure by a set of point charges optimized to reproduce its electrostatic field. Among the many possible ways to fit the electrostatic potential [39–42], we chose the CHelpG scheme as implemented in *Gaussian 09*. The Van der Waals exclusion radii used in fitting the potentials were those predefined in *Gaussian 09*, except for Br, where we used a VdW radium of 1.86 Å [43]. The iterative procedure required normally 9–12 iteration steps to achieve convergence on the orbital energies. (iii) The MO's of the whole molecule were projected on the MO's of the fragments.

3. Results

Compound (**I**) crystallizes in the C2/c space group, with one single molecule in the asymmetric unit. Since the analysis of its structure will greatly benefit from a comparison with the strongly related "parent" structure, 4-bromobenzoic acid (**II**) (CSD Refcode BRBZAP02), we present in Table 1 a summary of the crystallographic data for both compounds, while in Tables 2–5 we include a survey of (similar) non-covalent interactions present in both structures. Each interaction has been characterized by a special code, by which they will be referred to in the text and figures.

Bond lengths and angles in (**I**) are unexceptional, and the overall geometry departs only slightly from planarity, as demonstrated by the torsion angles involving pendant groups: (carboxy: $C_2-C_1-C_7-O_3$: −6.15(1)°; $C_6-C_1-C_7-O_4$: −4.10(1)°, methoxy: $C_6-C_5-O_2-C_9$: −0.49(1)°; $C_2-C_3-O_1-C_8$: −2.78(1)°). As expected for this type of molecules, the most interesting aspect of the structure derives from the non-covalent interactions responsible of the packing organization. In what follows special attention will be devoted to two of them: those of the O–H···O and Br···Br types, which constitute the driving forces generating the packing units in both structures.

The first one takes the form of head-to-head dimeric contacts (Table 2, #1a and #1b and Fig 1), and generate the well known $R_2^2(8)$ synthon observed in most of the benzoic acid derivatives reported so far. In both structures the interactions are strong and yield robust dimeric entities. Note in Fig 1 the disposition of the bromine atoms present in both dimers, protruding outwards at both ends.

This characteristic is responsible for the second significant interaction shared by (**I**) and (**II**) (labeled #6a and #5b in Table 3). The (type II) C–Br···Br–C halogen bonds therein presented give rise to an extremely similar, zig-zag pattern along the crystallographic b axis, with parallel dimeric units aligned in columnar arrays that run along [010] and columns at both sides of the zig-zag system that leave dimers at almost right angles to each other (Fig 2) and at *ca.* 50° to [010]. Since these dimers interact at both ends by means of their C–Br groups, the resulting concatenated substructures are basically 2D, yielding slabs parallel to (101) in (**I**) and to (−103) in (**II**).

It is at this stage where the presence of the methoxo substituents at 3,5 introduces a substantial difference. In (**II**) there is a relatively small steric hindrance restraining the dimers to align in an "in-plane" fashion (characterized by a rather small dihedral

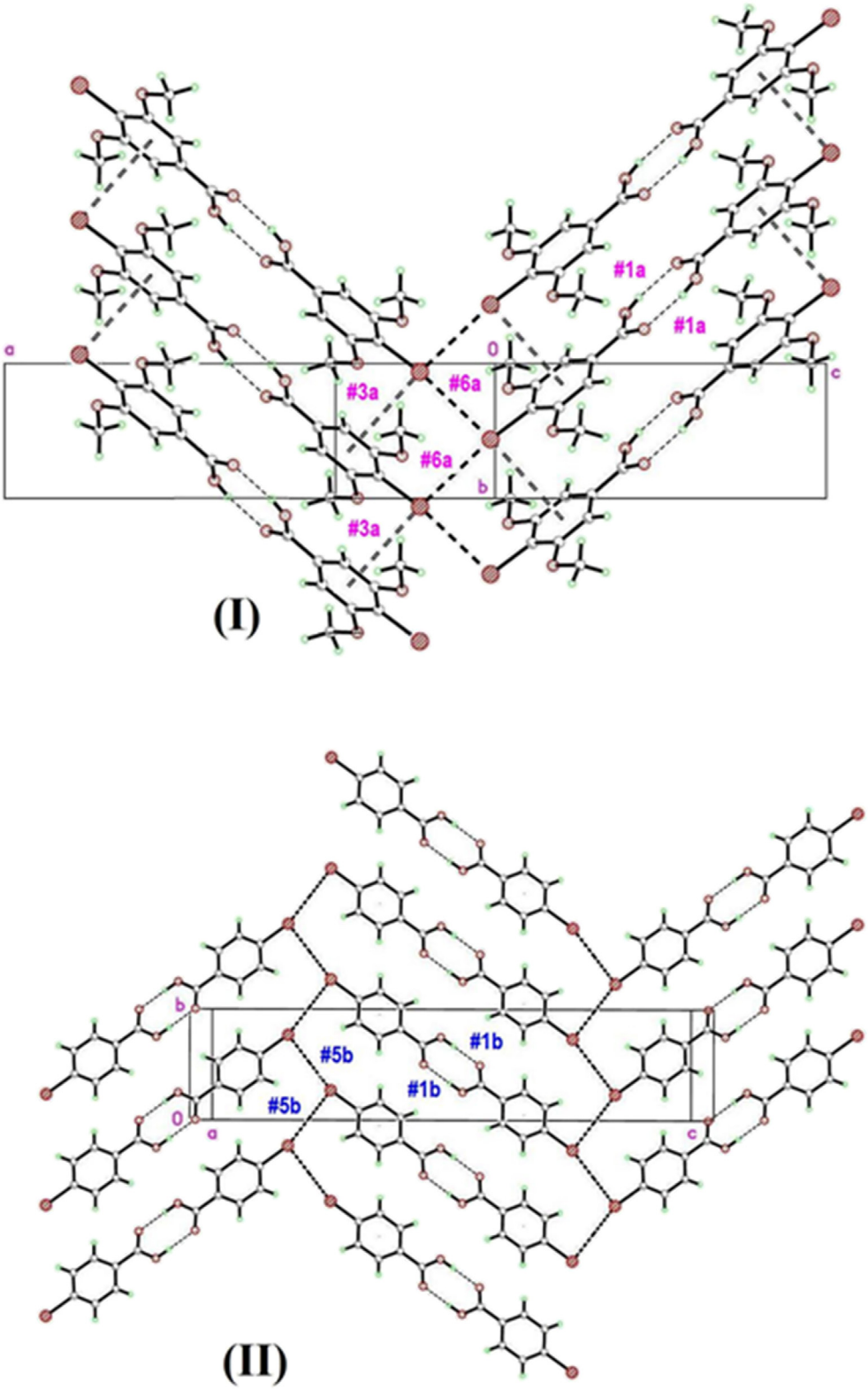

Fig. 2. The planar arrays in (**I**), (**II**), displaying the similar zig-zag motive generated by Br atoms. (For symmetry codes see Tables 2–5).

angle between the 2D structure and one single dimer: ~23.1°). On the contrary in the case of (**I**) the dimeric units have to rotate along their Br···Br line due to the neighbouring methoxy-groups. This rotation leads to a "nearly-perpendicular" disposition to the planar array, with a large dihedral angle (ca 61.5°) between the 2D structure and one single dimeric unit. This shows up in the "width" of the 2D slabs generated, as defined by the planes through the outermost non-H atoms, of approximately 6.30 Å in (**I**), in contrast with a much narrower 1.50 Å in (**II**) (Fig. 3, highlighted regions).

There are in addition a number of second order differences

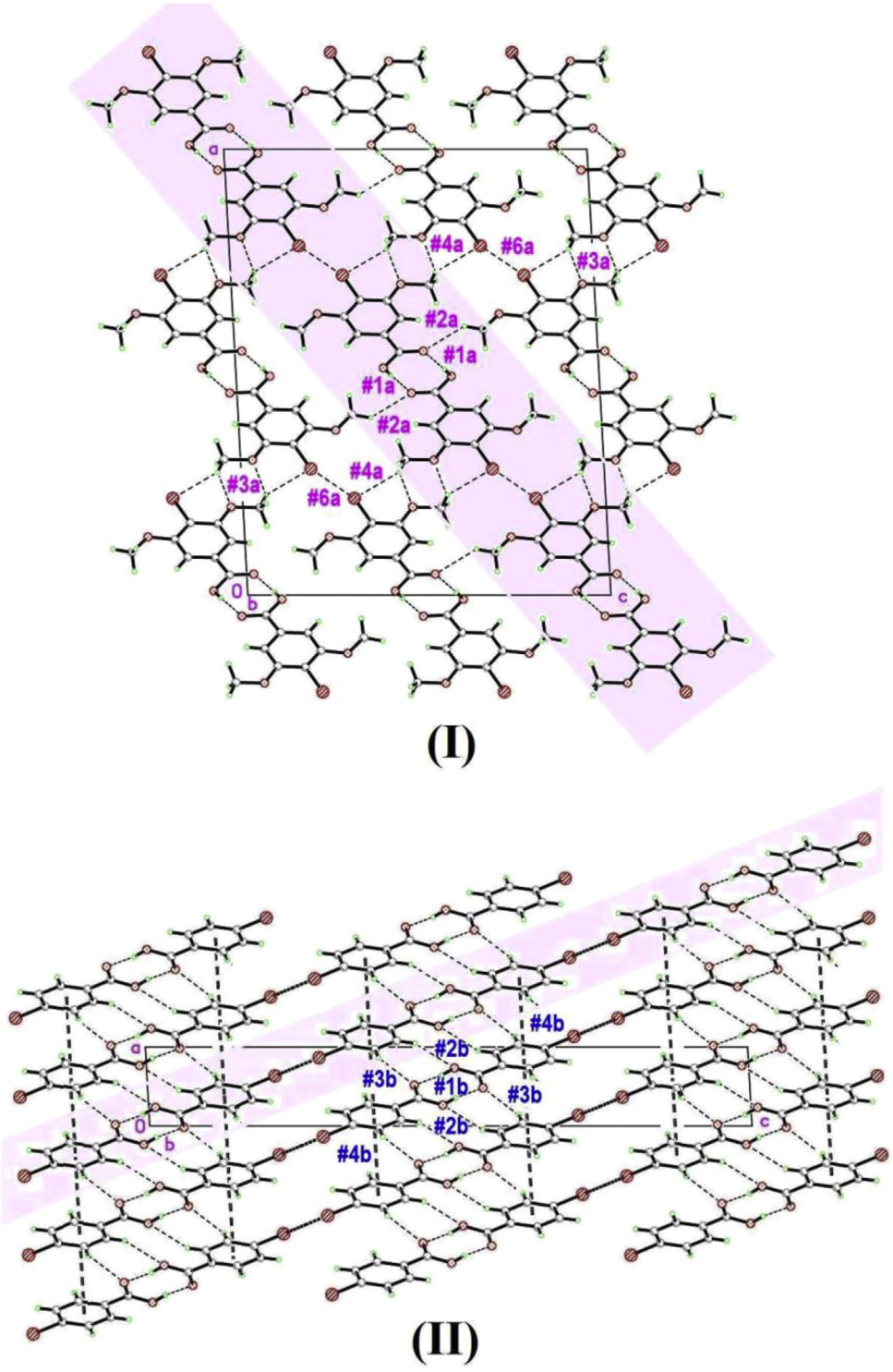

Fig. 3. - The 3D structures in (**I**), (**II**), with the arrays in Fig. 2 seen in projection (highlighted). (For symmetry codes see Tables 2–5).

derived from this diverse disposition of the dimers in the slabs. For instance, the usual stacking interaction involving aromatic rings is of different nature: C–Br ··· π in (**I**), (Table 3, #5a); π ··· π in (**II**) (Table 4, #4b). These interactions involve a different topology, being intra-planar in (**I**) (Fig. 2) but connecting slabs in (**II**) (Fig 3). The remaining interactions presented in Tables 2–5 mainly serve to link slabs together, as shown in Fig. 3.

4. Discussion

Following the general description of the packing interactions, we will focus on the C–Br ··· Br–C ones, #6a and #5b in Table 5. The comparison of (**I**) and (**II**) reveals geometrical similarities confirming the anticipated synthon modularity. The same kind of arrangement has been found in the crystalline form II of benzamide and several of its cocrystals with aliphatic diacids [24]. Inspection of

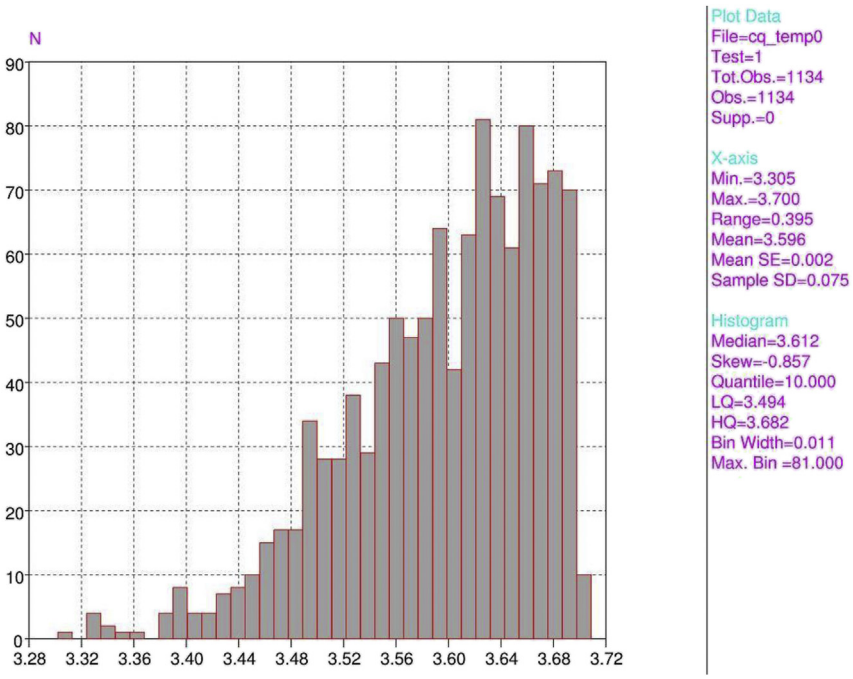

Fig. 4. - Distribution of Type II C–Br···Br–C contacts, as found in the CSD. Search criteria: 90° < C–Br···Br' < 135°; 135°<Br···Br'-C'<180°, R < 0.075, no disorder, no errors.

the values collected in Table 5 clearly shows a much shorter (meaningful) interaction distance in (**I**) than in (**II**). Fig. 4 represents the distribution of bondlengths for type II interactions of the same sort reported in the literature. While the Br ··· Br distance of 3.808A reported for (**II**) falls outside the commonly accepted range in the CSD, the 3.578(4)Å in (**I**) lays in the second quartile, slightly below the mean value of the distribution. Further comparisons with other 3,5- disubstituted 4-bromobenzoic acids of known structure (namely SEZGUA (3,5-dihydroxy-4-bromobenzoic acid) and TUSQUT (2,3,5,6-tetra(methyl)-4-bromobenzoic acid)) will not be conducted because none of them exhibits type II Br···Br contacts. In the first one, Br atoms are just involved in Br···OH and Br···O=C interactions; the second one corresponds to type I contacts with long Br···Br distance.

From a topological point of view, the possibility of a tighter Br ··· Br approach in **(I)** than in **(II)** has obviously to do with the particular disposition of the dimers in the slabs. A shorter Br···Br distance could be related to different electronic density distributions at the C–Br bonds in both compounds but also to a compromise between all the intermolecular interactions. A visual inspection of the structures does not univocally suggest that the shorter distance in (**II**) could be determined by other specific interactions. In order to evaluate more precisely this point, we performed SP-QM calculations on pairs of molecules at their experimental geometry and calculated the interaction energy (*E*) in each case, as described in the experimental section. Fig. 5 shows all the analyzed cases, describing the interactions involved in each case and the computed interaction energy. We performed these calculation on dimers of molecules instead of dimers of (head-to-head) dimers, both for simplicity and conceptual reasons. Nevertheless, we also calculated interactions energies (*E*) for dimers of dimers in the case of the X ··· X bond, and obtained nearly identical values, thus validating our simplifying calculation approach.

As expected, the strong hydrogen bond between carboxylic groups that gives rise to the head-to-head dimers (#1a and #1b) is the prevalent interaction, with *ca.* 25 kJ/mol per interaction. The π interactions #5a and #4b at *ca.* 26 kJ/mol are of comparable strength. Halogen bond interactions #6a and #5b at ca. 4.5 kJ/mol (that is within the range found in Ref. [23]) are comparable to the weak H-bond interactions C–H···O and C–H···Br (#2a, #2b, #3a, #3b, #4a), which are in the range 0–12 kJ/mol per individual interaction. In agreement with the different Br···Br distances in (**I**) to (**II**), the corresponding interacting energies differ by *ca.* 25%. In what follows we attempt to disclose the effect exerted by the methoxy-groups on this particular interaction. The effect of substituents on the strength of $R_{don}C$-X ··· Nu-R_{acc} XBs has often been analyzed in terms of the ability of the substituents on the R_{don} fragment to attract electron density. An increase of the positive electrostatic potential ($V_{s,max}$) at the "σ-hole" on the X atom would yield this atom more electrophilic [3,7,18,44]. Alternatively, the electron-donor ability of the substituents on N- or O-containing Nu-R_{acc} groups has also been correlated with the Nu basicity, and then to its tendency to bind to R_{don}-X [3,18–21]. In the present case, the base interacting with the σ–hole on Br is also a Br atom from an identical molecule, but with a near perpendicular orientation. The effect of methoxy-groups (π-electron donors) on electron density distribution will operate simultaneously on R_{don}-X and Nu-R_{acc}; in the later case, it should mainly manifest as an increased electron density in the belt perpendicular to the C–Br bond of the Nu-R_{acc} (base) moiety.

In order to confirm this expectation based on usual qualitative chemical arguments, we performed quantum mechanical calculations aimed to assess the electronic distributions on both (**I**) and (**II**) molecules. The results of these calculations, presented in the form of the electrostatic potential projected on the molecular surface, are represented on Fig. 6.

The electrostatic potential map of (**I**) reveals a significant decrease on the Br atom, in a plane perpendicular to the C–Br bond (the "belt"), consistent with an augmented electron density on this region of the space. Based on electrostatic considerations, this Br atom (Nu), which is oriented in a near-perpendicular fashion with respect to the Br–C bond in the X-donor moiety, would act as a stronger base than in the case of (**II**). This fact could give rise, in principle, to the significantly shorter Br ··· Br distance. However,

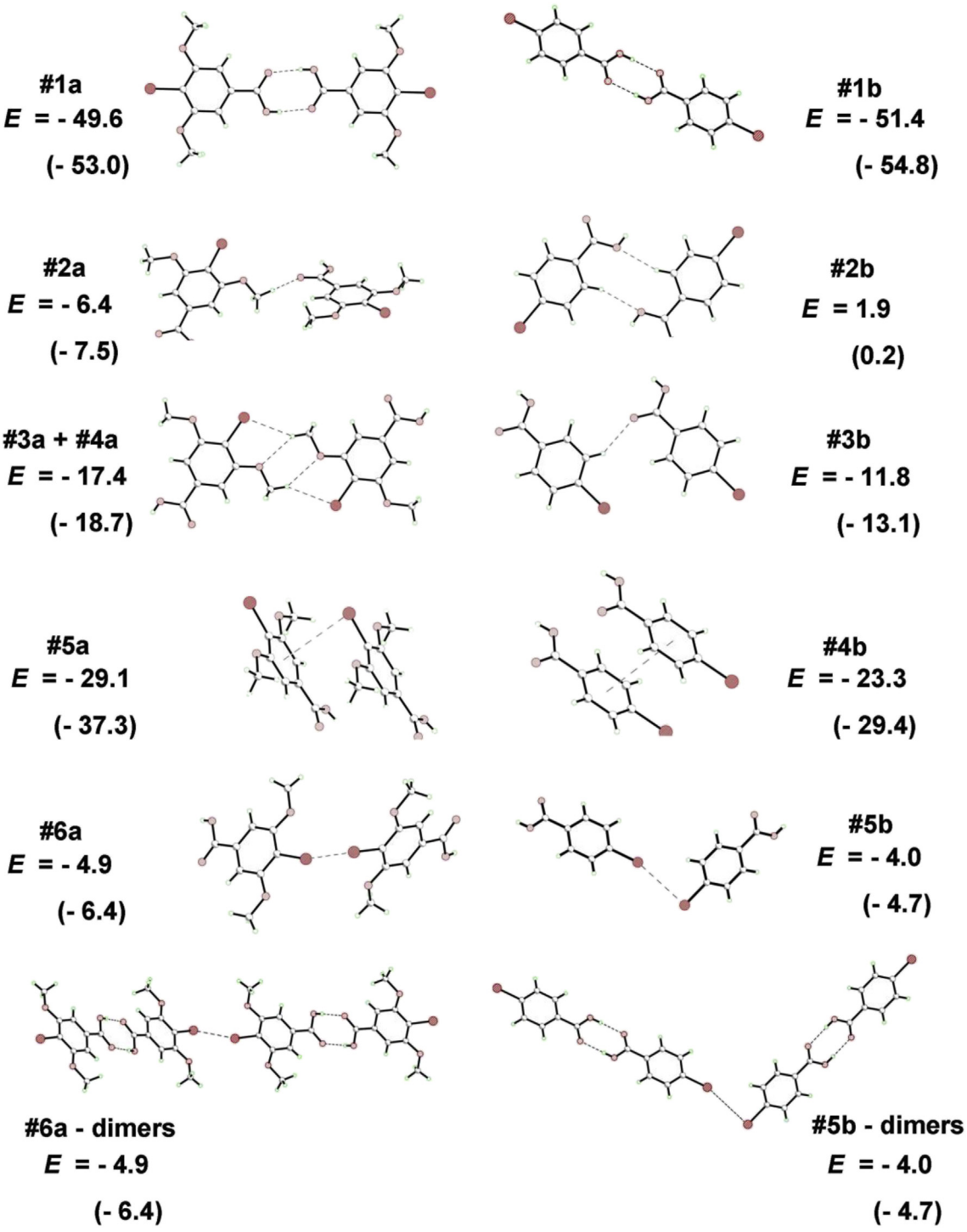

Fig. 5. Counterpoise-corrected interaction energies in kJ/mole for pairs of molecules of (I) (left) and (II) (right) selected in such a way that each pair involves just one or two specific interactions. Numbers in parenthesis do not involve corrections for the basis set superposition errors (BSSE).

methoxy groups also affect the electron density at the σ-hole and indeed, a less positive σ-hole is found for (**I**) than for (**II**). A complete discussion requires a closer inspection of the electrostatic potential maps projected on the molecular surface (V_S maps); such analysis shows the following significant features: i) the local maximum of V_s ($V_{s,max}$) on the electrophile is located in both cases at the σ-hole, and is more positive for (**II**) than for (**I**) (0.024 *vs.* 0.013 a.u. respectively). ii) The local minimum of V_s ($V_{s,min}$) is located on different regions of the nucleophile in (**I**) and (**II**): it is found on a position of the belt nearly perpendicular to the benzoic plane in (**II**), but on an intermediate point between Br and O atoms in the case of (**I**). iii) $V_{s,min}$ is significantly more negative for (**I**) than for (**II**): −0.047 a.u. for the former *vs.* −0.013 a.u. for the later. iv) $V_{s,max}$ - $V_{s,min}$ −a parameter usually associated with the strength of electrostatically driven X ··· X type II contacts, and successfully employed to rationalize tendencies in nearly colinear (C-X ··· Nu)

Table 1
Crystallographic parameters for (I), (II).

	(I)[a]	(II)[b]
Crystal data		
Chemical formula	$C_9H_9BrO_4$	$C_7H_5BrO_2$
M_r	261.07	201.01
Crystal system, space group	Monoclinic, *C*2/*c*	Monoclinic, $P2_1/n$
Temperature (K)	170	198
a, *b*, *c* (Å)	22.3405 (6), 4.85142 (14), 18.1583 (5)	3.888 (1), 6.068 (1), 29.190 (1)
β (°)	93.086 (2)	92.86 (1)
V (Å^3)	1965.20 (9)	687.80
Z	8	4
$R[F^2 > 2\sigma(F^2)]$	0.035	0.043
R_{int}	0.050	
μ (mm^{-1})	4.17	
No. of measured, independent and observed reflections	11138, 2365, 2075 [$I > 2\sigma(I)$]	

[a] this work.
[b] CSD REFCODE: BRBZAP02 (M.Albrecht,A., Schmid,S. & Frohlich,R., Private Communication, 2004 Private Communication (2004).

Table 2
Hydrogen bonds for **(I)** and **(II)** [Å and °].

Comp.	Code	D-H...A	d(D-H)	d(H … A)	d(D … A)	<(DHA)
(I)						
	#1a	$O_3\cdots H_3O\cdots O_4^{(i)}$	0.846(1)	1.787(14)	2.622(3)	168(5)
	#2a	$C_8\cdots H_8B\cdots O_4^{(ii)}$	0.96	2.64	3.398(4)	136
	#3a	$C_9\cdots H_9A$ … $O_2^{(iii)}$	0.96	2.63	3.447(4)	143
	#4a	$C_9—H_9A$ … $Br_1^{(iv)}$	0.96	2.98	3.859(3)	153
(II)						
	#1b	$O_3\cdots H_3O\cdots O_4^{[i]}$	0.80(5)	1.83(5)	2.622(3)	172(5)
	#2b	$C_2\cdots H_2\cdots O_3^{[ii]}$	0.95	2.52	3.407(4)	156
	#3b	$C_3\cdots H_3\cdots O_4^{[iii]}$	0.95	2.53	3.329(4)	142

Symmetry codes for (I) (i)-x,-1-y,1-z; (ii) x,-y,-1/2 + z; (iii) 1/2-x,3/2-y,1-z; (iv) 1/2-x,1/2-y,-z.
Symmetry codes for (II) [i]1-x,1-y,1-z; [ii] -x,2-y,1-z; [iii] −1+x,1 + y,z.

systems [2,12]- is significantly higher for (**I**) than for (**II**) (0.060 vs. 0.037 a.u. respectively). In our case, the value of $V_{s,max}$ - $V_{s,min}$ couldn't be employed to explain the closer Br···Br contact in (**I**). Indeed, the electrostatic potential maps for both (**I**) and (**II**) depicted in Fig. 6 show that the σ-hole is not strictly oriented towards $V_{s,min}$ but to regions in the vicinity of this point. This fact suggests an overall compromise between intrinsic factors associated to the XB interaction and the geometric requirements of the other operating interactions. An estimation of $V_{s,cont}$, the electrostatic potentials V_s for individual monomers evaluated at the contact point, yields a potential difference $V_{s,cont,\ electrophile} - V_{s,cont,\ nucleophile}$ of approximately 0.045 a.u for (**I**) and 0.030 a.u. for (**II**), a difference in line with the shorter Br···Br approach in (**I**).

Complementary, we undertook MO calculations on pairs of

Table 3
C-X … π contacts.

Comp.	Code	C-X … Cg	d(C-X) (Å)	d(X … Cg) (Å)	d<(CXCg) °	<(CX-perp)>°
(I)						
	#5a	$C_4—Br_1$ … $Cg_1^{(v)}$	1.881(3)	3.857(2)	84.76(8)	2.1
(II)						
	None					

Symmetry codes for (I) (v) x,1 + y,z.

Table 4
π … π contacts.

Comp.	Code	Cg … Cg	d(Cg … Cg) (Å)	da (°)	ipd (Å)	sd (Å)
(I)						
	None					
(II)						
	#4b	Cg1 … Cg1$^{[iv]}$	3.854(2)	0	3.470(2)	1.677(2)

da: dihedral angle; ipd. interplanar distance, sp: slipage distance.
Symmetry codes for (II) [iv] 1 + x,y,z.

Table 5
Halogen bonds.

Comp.	Code	C-X...X′-C′	d(X … X) (Å)	<CXX'> (°)	<XX'C'> (°)
(I)					
	#6a	$C_4—Br_1$ … $(Br_1—C_4)^{(vi)}$	3.5779(5)	98.3	163.0
(II)					
	#5b	$C_4—Br_1$ … $(Br_1—C_4)^{[v]}$	3.808	91.6	163.5

Symmetry codes for (I) (vi) 1/2-x,1/2 + y,1/2-z.
Symmetry codes for (II) [v] −1/2-x, 1/2 + y, 1/2-z.

Br···Br interacting molecules of (**I**) and (**II**), in order to reveal any additional covalent interactions contributing to the XB bond. The computations were performed at the geometry found in the respective crystals, and the results were analyzed in terms of the individual contribution of the molecular orbitals of the fragments to the MO scheme. A very weak interaction is revealed in both cases (Fig. 7), giving rise to delocalized frontier MOs. However, it should be stressed out that the HOMO-LUMO gap is very low in agreement with the almost negligible overlap coefficients. Moreover, there are no significant differences between (**I**) and (**II**).

5. Conclusions

The type II Br ··· Br interaction has been found to be an efficient organizer of the head-to-head dimeric synthons in the substituted bromo-benzoic acid (**I**) due to the presence of substituents that enhance the electron density in the appropriate molecular region. The inclusion of methoxy-substituents on Nu-R_{acc} appears as a valuable strategy for the design of type II XB-based supramolecular arrangements (a subject still under debate) even in the presence of other non-covalent interactions. Some additional evidence of the

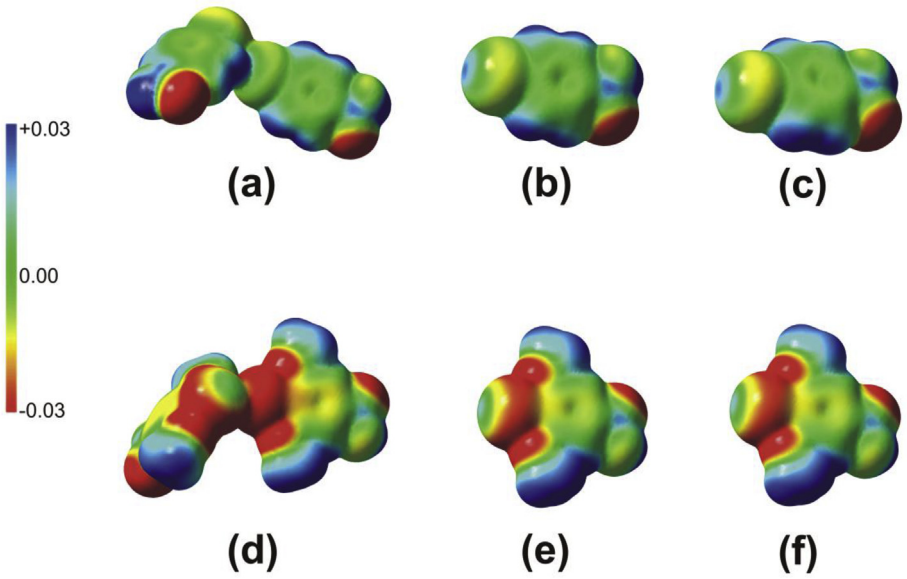

Fig. 6. – Electrostatic potential maps at the molecular surface for 4-Bromobenzoic acid (**II**) (top) and 4-Bromo-3,5-di(methoxy)benzoic acid (**I**) (bottom). The representations correspond to a cut off of 0.001 e/bohr^3 for the electron density. The color-scale of electrostatic potential is given in atomic units. From left to right the plots correspond to the interacting pairs ((a) and (d)), the free units ((b) and (e)) and the latter immersed in the electric field induced by their counterparts((e) and (f)).

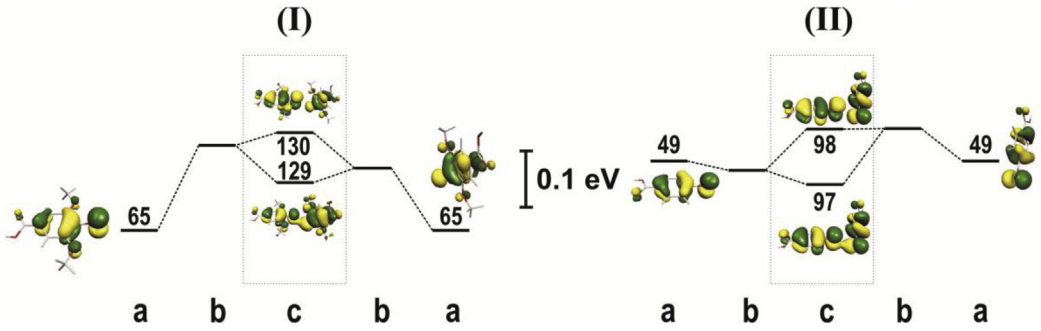

Fig. 7. Frontier MO diagrams for both (**I**) (left) and (**II**) (right). **(a)** represents the MO energy for the isolated molecules, **(b)** shows the electronic structure of the molecules in the presence of the electrostatic potential generated by the complementary fragment, and **(c)** represents the MO picture for the dimers.

essentially electrostatic nature of this interaction in the present case has been found by means of QM calculations of the electrostatic potential. A fragment based molecular orbital analysis performed on (**I**) and (**II**) reveals a very weak covalent component that does not contribute significantly to the whole interaction. This MO decomposition methodology could be extended to other systems, including those with stronger XB. The organizing ability of this kind of XB in cocrystals based on tricomponent synthons (brominated acid – dinitrogenated base – brominated acid) looks promising in order to get a deeper understanding of the transferability of this motif in the context of crystal engineering. Both kinds of studies are systematically being carried out in our labs and will be the subject of further reports.

Acknowledgements

We acknowledge ANPCyT (grant PME 01113 for X-ray diffractometer), UBACyT (grant 20020130100776BA), CONICET (grant PIP 0659 and PhD fellowships for PR and AF), the National Center for Supercomputing Applications (grant TG-MCA05S010) and INQUIMAE (CSD license) for financial support. LDS and FDC are members of the research staff of Conicet.

References

[1] P. Metrangolo, F. Meyer, T. Pilati, G. Resnati, G. Terraneo, Angew. Chem. Int. Ed. 47 (2008) 6114–6127.
[2] L.C. Gilday, S.W. Robinson, T.A. Barendt, M.J. Langton, B.R. Mullaney, P.D. Beer, Chem. Rev. 115 (2015) 7118–7195.
[3] P. Politzer, J.S. Murray, ChemPhysChem 14 (2013) 278–294.
[4] G.R. Desiraju, J. Am. Chem. Soc. 135 (2013) 9952–9967.
[5] A. Priimagi, G. Cavallo, P. Metrangolo, G. Resnati, Acc. Chem. Res. 46 (2013) 2686–2695.
[6] M. Fourmigué, Curr. Opin. Solid State Mater. Sci. 13 (2009) 36–45.
[7] C.B. Aakeroy, M. Baldrighi, J. Desper, P. Metrangolo, G. Resnati, Chem. Eur. J. 19 (2013) 16240–16247.
[8] S.V. Rosokha, C.L. Stern, J.T. Ritzert, Chem. Eur. J. 19 (2013) 8774–8788.
[9] P. Metrangolo, G. Resnati, T. Pilati, R. Liantonio, F. Meyer, J. Polym. Sci. Part A 45 (2007) 1–15.
[10] A. Mukherjee, G.R. Desiraju, IUCrJ 1 (2014) 49–60.
[11] A. Takemura, L.J. McAllister, P.B. Karadakov, N.E. Pridmore, A.C. Whitwood, D.W. Bruce, CrystEngComm 16 (2014) 4254–4264.
[12] P. Politzer, J.S. Murray, T. Clark, Phys. Chem. Chem. Phys. 15 (2013) 11178–11189.
[13] H. Li, Y. Lu, Y. Liu, X. Zhu, H. Liu, W. Zhu, Phys. Chem. Chem. Phys. 14 (2012) 9948–9955.
[14] J.-Y. Le Questel, C. Laurence, J. Graton, CrystEngComm 15 (2013) 3212–3221.
[15] M.D. Esrafili, M. Vakili, M. Solimannejad, J. Mol. Model 20 (2014) 2102.
[16] S.J. Grabowski, Phys. Chem. Chem. Phys. 15 (2013) 7249–7259.
[17] B. Pinter, N. Nagels, W.A. Herrebout, F. De Proft, Chem. Eur. J. 8 (2013) 519–530.
[18] A. Bauzá, D. Quiñonero, A. Frontera, P.M. Deyà, Phys. Chem. Chem. Phys. 13

(2011) 20371–20379.
[19] K.E. Riley, J.S. Murray, J. Fanfrlik, J. Rezak, R.J. Sola, M.C. Concha, F.M. Ramos, P. Politzer, J. Mol. Model. 17 (2011) 3309–3318.
[20] M. Tawfik, K.J. Donald, J. Phys. Chem. A 118 (43) (2014) 10090–10100.
[21] W. Wu, Y. Lu, Y. Liu, C. Peng, H. Liu, Comput. Theor. Chem. 1029 (2014) 21–25.
[22] T. Thanh, T. Bui, S. Dahaoui, C. Lecomte, G.R. Desiraju, E. Espinosa, Angew. Chem. Int. Ed. 48 (2009) 3838–3841.
[23] M. Capdevila-Cortada, J.J. Novoa, CrystEngComm 17 (2015) 3354–3365.
[24] P. Metrangolo, G. Resnati, IUCrJ 1 (2014) 5–7.
[25] S. Tothadi, S. Joseph, G.R. Desiraju, Cryst. Growth Des. 13 (2013) 3242–3254.
[26] K. Ohkura, S. Kashino, M. Haisa, Bull. Chem. Soc. Jpn. 45 (1972) 2651–2652.
[27] P.A. Raffo, L. Rossi, P. Alborés, R.F. Baggio, F.D. Cukiernik, J. Mol. Struct. 1070 (2014) 86–93.
[28] G.R. Desiraju, K.V.R. Kishan, J. Am. Chem. Soc. 111 (1989) 4838–4843.
[29] P. Kirsop, J.M.D. Storey, W.T.A. Harrison, Acta Cryst. E63 (2007) o1441–o1443.
[30] Oxford Diffraction, CrysAlis PRO, Oxford Diffraction Ltd, Yarnton, Oxfordshire, England, 2009.
[31] G.M. Sheldrick, Acta Cryst. A 64 (2008) 112–122.
[32] G.M. Sheldrick, Acta Cryst. C 71 (2015) 3–8.
[33] A.L. Spek, Acta Cryst. D. 65 (2009) 148–155.
[34] M.J. Frisch, Gaussian 09, Rev. A.02 and D.01, Gaussian Inc., Wallingford CT, 2009.
[35] H.B. Jansen, P. Ros, Chem. Phys. Lett. 3 (1969) 140.
[36] B. Liu, A.D. McLean, J. Chem. Phys. 59 (1973) 4557.
[37] S.F. Boys, F. Bernardi, Mol. Phys. 19 (1970) 553.
[38] S. Simon, M. Duran, J.J. Dannenberg, J. Chem. Phys. 105 (1996) 11024–11031.
[39] B.H. Besler, K.M. Merz Jr., P.A. Kollman, J. Comp. Chem. 11 (1990) 431.
[40] L.E. Chirlian, M.M. Francl, J. Comp. Chem. 8 (1987) 894.
[41] U.C. Singh, P.A. Kollman, J. Comp. Chem. 5 (1984) 129.
[42] C.M. Breneman, K.B. Wiberg, J. Comp. Chem. 11 (1990) 361.
[43] S. Alvarez, Dalton Trans. 42 (2013) 8617–8636.
[44] K.E. Riley, J.S. Murray, P. Politzer, M.C. Concha, P. Hobza, J. Chem. Theory Comput. 5 (2009) 155–163.